AD-A061 327 NAVAL OCEAN SYSTEMS CENTER SAN DIEGO CA F/G 14/2
MTI FOLLOWED BY INCOHERENT INTEGRATION-AN EXACT ANALYSIS.(U)
SEP 78 G M DILLARD, D M KLAMER, J T RICKARD

UNCLASSIFIED NOSC/TR-311 NL

| OF |
AD
A061327

END
DATE
FILMED
2 - 79
DDC

NOSC

NOSC TR 311

(9) Technical Report 311

(6)

MTI FOLLOWED BY INCOHERENT INTEGRATION—AN EXACT ANALYSIS

(10) G.M. Dillard (NOSC)
D.M. Klamer (NOSC)
J.T. Rickard (ORINCON)

(11) 14 September 1978

(12) 33 p.

(14) NOSC/TR-311

NAVAL OCEAN SYSTEMS CENTER
SAN DIEGO, CALIFORNIA 92152

NAVAL OCEAN SYSTEMS CENTER, SAN DIEGO, CA 92152

AN ACTIVITY OF THE NAVAL MATERIAL COMMAND

RR GAVAZZI, CAPT, USN
Commander

HL BLOOD
Technical Director

ADMINISTRATIVE INFORMATION

This work was completed by the Tactical Command Control Division, Code 8242, Naval Ocean Systems Center.

Released by
RC Kolb, Head
Tactical Command Control
Division

Under authority of
JH Maynard, Head
Command Control-Electronic
Warfare Systems and
Technology Department

NAVAL OCEAN SYSTEMS CENTER
San Diego, California 92152
27 November 1978

NOSC Technical Report TR 311

MTI FOLLOWED BY INCOHERENT INTEGRATION – AN EXACT ANALYSIS,
by GM Dillard (NOSC), DM Klamer (NOSC), and JT Rickard (ORINCON),
14 September 1978

LITERATURE CHANGE

Please make the following changes to your copy of NOSC TR 311:

1. On page 19, delete everything following equation (24b).
2. On page 19, add following text after equation (24b):

   Now, g_k^2 can be determined by using (21) and (24).
3. On page 20, delete all text above APPLICATIONS TO OVERLAPPING DFT'S.
4. On cover, below 14 September 1978, add:

   Changed 27 November 1978.

UNCLASSIFIED

SECURITY CLASSIFICATION OF THIS PAGE (When Data Entered)

REPORT DOCUMENTATION PAGE		READ INSTRUCTIONS BEFORE COMPLETING FORM
1. REPORT NUMBER NOSC Technical Report 311 (TR311)	2. GOVT ACCESSION NO.	3. RECIPIENT'S CATALOG NUMBER
4. TITLE (and Subtitle) MTI FOLLOWED BY INCOHERENT INTEGRATION – AN EXACT ANALYSIS		5. TYPE OF REPORT & PERIOD COVERED Interim – Current
		6. PERFORMING ORG. REPORT NUMBER
7. AUTHOR(s) GM Dillard and DM Klamer (NOSC) and JT Rickard (ORINCON)		8. CONTRACT OR GRANT NUMBER(s)
9. PERFORMING ORGANIZATION NAME AND ADDRESS Naval Ocean Systems Center (NOSC) San Diego, California 92152		10. PROGRAM ELEMENT, PROJECT, TASK AREA & WORK UNIT NUMBERS Internally funded
11. CONTROLLING OFFICE NAME AND ADDRESS NOSC		12. REPORT DATE 14 September 1978
		13. NUMBER OF PAGES 28
14. MONITORING AGENCY NAME & ADDRESS(if different from Controlling Office)		15. SECURITY CLASS. (of this report) Unclassified
		15a. DECLASSIFICATION/DOWNGRADING SCHEDULE

16. DISTRIBUTION STATEMENT (of this Report)

Approved for public release; distribution unlimited

17. DISTRIBUTION STATEMENT (of the abstract entered in Block 20, if different from Report)

18. SUPPLEMENTARY NOTES

19. KEY WORDS (Continue on reverse side if necessary and identify by block number)

Algorithms – Numerical integration
Correlation techniques
Detection
Moving target indicator
Threshold effects

20. ABSTRACT (Continue on reverse side if necessary and identify by block number)

Provides an exact computational method (and the associated theory) for determining the detection threshold to be used when a square-law integrator is applied to the output from a nonrecursive MTI. Using this method, a table of bias levels is computed for a two-pulse (single-delay) MTI for several values of the number N of pulses integrated and the probability PFA of a false alarm. Derives the characteristic function of the output of the square-law integrator when the MTI input contains a signal with Doppler frequency f_d and amplitude G.

Gives the general theory for obtaining the characteristic function of the sum of squared magnitudes of correlated, circular-Gaussian random variables. Discusses in detail the application of the general theory to the computation of bias levels for a nonrecursive MTI. (cont)

DD FORM 1 JAN 73 1473 EDITION OF 1 NOV 65 IS OBSOLETE
S/N 0102-014-6601 |

UNCLASSIFIED

SECURITY CLASSIFICATION OF THIS PAGE (When Data Entered)

Briefly considers applications to signal detection based on incoherent integration of overlapping discrete Fourier transforms.

OBJECTIVE

Develop and analyze advanced signal processing techniques that will provide improved performance, reliability, and maintainability while reducing costs of signal processing systems for radar, sonar, and electronic warfare.

RESULTS

1. An exact computational method is given for determining the detection threshold to be used when a square-law integrator is applied to the output from a nonrecursive moving target indicator (MTI).

2. A table of bias levels is given for a two-pulse (single-delay) MTI for several values of the number N of pulses integrated and the probability PFA of a false alarm.

3. The characteristic function of the output from the square-law integrator is determined for the case where the MTI input contains a signal.

RECOMMENDATION

Continue the analysis of the effect of MTI on incoherent integration. Specifically, determine exact (or approximate) methods for computing detection probabilities, and investigate optimum methods for constant false-alarm rate (CFAR) processing for an MTI followed by incoherent integration.

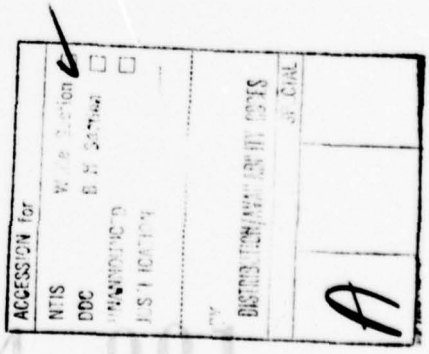

BACKGROUND

This report describes the results of work that is in progress at the Naval Ocean Systems Center (NOSC), San Diego, California, and at ORINCON Corporation, La Jolla, California. Further results will be described in an expanded version of this report which will be submitted for publication in the IEEE Transactions on Aerospace and Electronic Systems.

INTRODUCTION

The output sequence from a nonrecursive MTI is a linear combination of the inputs from successive pulse repetition intervals (PRI's). Thus, the sequence at the MTI output is correlated even though the input sequence may be uncorrelated. When detection is performed by incoherent integration of successive MTI outputs (for each range bin), the variables integrated are not statistically independent. This poses two problems. First, the determination of the detection threshold must take into account the noise correlation, and thus graphs or tables of thresholds (e.g., Pachares' table [1]) previously published cannot be used. Second, the noise correlation degrades detection performance, as has been indicated in the literature [2,3,4]. Trunk [2] considered both problems and obtained detection thresholds and detection sensitivity, by Monte Carlo simulation, for a linear integrator at the output of a binary-weighted MTI. Hall and Ward [3] and Kretschmer [4] estimated the detection sensitivity degradation for a square-law integrator by computing the "effective number" N_e of pulses from a ratio of variances and squared means.

This report serves two purposes. The first is to provide an exact computational method (and the associated theory) for determining the detection threshold to be used when a square-law integrator is applied to the output from a nonrecursive MTI. Using this method, a table of bias levels is computed for a two-pulse (single-delay) MTI for several values of the number N of pulses integrated and the probability PFA of a false alarm.

The second purpose is to derive the characteristic function of the output of the square-law integrator when the MTI input contains a signal with Doppler frequency f_d and amplitude G. While inversion of this characteristic function (to find the associated probability density) has proven to be intractable, the techniques of Helstrom [5] can be used to estimate the detection probability.*

The general theory is given for obtaining the characteristic function of the sum of squared magnitudes of correlated, circular-Gaussian [6] random variables. (The particular circular-Gaussian process considered here corresponds to the in-phase and quadrature components of the complex envelope of a Gaussian stochastic process.) For the case where the variables have zero mean (i.e., the no-signal case), the characteristic function is inverted, and the probability distribution is obtained. The application of the general theory to the computation of bias

---

*Estimates of the detection probability will be given in the journal publication which will follow at a later date. Comparisons will then be made with the estimates of Hall and Ward [3] and the simulation results of Trunk [2].

levels for a nonrecursive MTI is discussed in detail. Also, applications to signal detection based on incoherent integration of overlapping discrete Fourier transforms (DFT's) are considered briefly.

The theory given here is similar to derivations by other authors, such as Kac and Siegert [7], Emerson [8], and Meyer and Middleton [9]. For example, Kac and Siegert [7] obtained the characteristic function of the (unsampled) output from a video amplifier which follows a square-law detector, and expressed their results in terms of eigenvalues and eigenfunctions of an integral equation. Emerson [8] considered the same problem and outlined procedures for determining probability density functions directly without solving the eigenvalue problem or inverting the characteristic function. Meyer and Middleton [9] extended the results of Kac and Siegert and obtained an explicit solution for the integral equation involving the autocorrelation function of the noise. Our work differs from these previous analyses in that we approach the problem from a sampled-data viewpoint and develop an exact computational method which provides a straightforward means of analyzing the performance of digital detection processors which employ incoherent integration of correlated random variables.

NONRECURSIVE MTI

For each range bin, the output from a nonrecursive MTI is a linear combination of the inputs from L successive pulse repetition intervals (PRI's). That is, the complex MTI output E_k is*

---

*The output is a complex variable obtained from the in-phase and quadrature components. The index k denotes the PRI; the index that would denote the range bin has been suppressed.

$$E_k = \sum_{\ell=1}^{L} W_\ell \, G_{k-\ell+L} \triangleq X_k + iY_k \qquad (1)$$

where $W_1, W_2, \ldots, W_L$ are fixed weights which, for this analysis, are assumed to be real. The real and imaginary parts of the input sequence $G_1, G_2, \ldots,$ are assumed to be independent normally distributed random variables with variance σ^2, and with means $m_1, m_2, \ldots,$ and $C_1, C_2, \ldots,$ respectively. Thus, the output $E_k \triangleq X_k + iY_k$, $k = 1,2, \ldots,$ is such that X_k and Y_k are normally distributed with means

$$\mu_k \triangleq E[X_k] = \sum_{\ell=1}^{L} W_\ell \, m_{k-\ell+L} \qquad (2)$$

$$\gamma_k \triangleq E[Y_k] = \sum_{\ell=1}^{L} W_\ell \, C_{k-\ell+L}$$

and with covariances

$$E[X_k X_{k+n} - \mu_k \mu_{k+n}] = E[Y_k Y_{k+n} - \gamma_k \gamma_{k+n}] = \begin{cases} \sigma^2 \displaystyle\sum_{\ell=1}^{L-n} W_\ell W_{\ell+n} & n<L \\ 0 & n \geq L \end{cases} \qquad (3a)$$

and

$$E[X_k Y_{k+n} - \mu_k \gamma_{k+n}] = 0 \qquad (3b)$$

$n=0,1,2,\ldots$

THEORY

With $X_1, X_2, \ldots, X_N$ and $Y_1, Y_2, \ldots, Y_N$ defined as above, their joint probability density is given by

$$f(\underline{x},\underline{y}) = (2\pi)^{-N}|A|\exp\left\{-\frac{1}{2}\left[(\underline{x}-\underline{\mu})A(\underline{x}'-\underline{\mu}')+(\underline{y}-\underline{\gamma})A(\underline{y}'-\underline{\gamma}')\right]\right\} \tag{4}$$

where A is the inverse of the covariance matrix R determined by (3a); $\underline{x}$, $\underline{y}$, etc., denote N-dimensional row vectors; $\underline{x}'$, $\underline{y}'$, etc., are their transposes (column vectors); and $|A|$ is the determinant of the matrix A.

From Kendall and Stuart [10, page 347], there is an orthogonal matrix (i.e., transformation) T such that $T'AT = D$, where D is a diagonal matrix. Also, the elements on the diagonal of D are the eigenvalues of A [11, page 186]. Applying this transformation T to $\underline{x}$ and $\underline{y}$ (by letting $\underline{x}' = T\underline{z}'$ and $\underline{y}' = T\underline{w}'$), the new variables $\underline{z}$ and $\underline{w}$ have joint density

$$f(\underline{z},\underline{w}) = (2\pi)^{-N}|D|\exp\left\{-\frac{1}{2}[(\underline{z}-\underline{\alpha})D(\underline{z}'-\underline{\alpha}')+(\underline{w}-\underline{\beta})D(\underline{w}'-\underline{\beta}')]\right\}\ , \tag{5}$$

where $\underline{\mu}' = T\underline{\alpha}'$ and $\underline{\gamma}' = T\underline{\beta}'$.

Note that since T is orthogonal,

$$S \triangleq \sum_{k=1}^{N} x_k^2 + y_k^2 = \underline{x}\,\underline{x}' + \underline{y}\,\underline{y}' = \underline{z}T'T\underline{z}' + \underline{w}T'T\underline{w}' = \sum_{k=1}^{N} w_k^2 + z_k^2\ . \tag{6}$$

From (6) and the discussion in the previous section, it follows that S can be interpreted as the result of square-law integration of N outputs from a nonrecursive MTI. We now determine the characteristic function of S from the joint density (5).

The change of variables $z_k = r_k \cos \theta_k$ and $w_k = r_k \sin \theta_k$ in (5) and integration with respect to $\theta_1, \theta_2, \ldots, \theta_N$ gives the joint density of $r_1, r_2, \ldots, r_N$:

$$f(\underline{r}) = \prod_{k=1}^{N} d_k r_k \exp\left\{-\frac{d_k}{2}\left(r_k^2 + g_k^2\right)\right\} I_0(d_k r_k g_k) \tag{7}$$

where $g_k^2 \triangleq \alpha_k^2 + \beta_k^2$, the d_k's are the eigenvalues of A, and $I_0(\cdot)$ is the modified Bessel function of the first kind, order zero. Finally, letting $q_k = r_k^2$, the joint density of $q_1, q_2, \ldots, q_N$ is

$$f(\underline{q}) = \prod_{k=1}^{N} \frac{d_k}{2} \exp\left\{-\frac{d_k}{2}\left(q_k + g_k^2\right)\right\} I_0(g_k d_k \sqrt{q_k}). \tag{8}$$

From (8) it follows that $q_1, q_2, \ldots, q_N$ are independent random variables; also, the transformations above are such that

$$S = \sum_{k=1}^{N} q_k .$$

Thus, the characteristic function (ch. f.) of S is given by

$$\phi_S(\omega) = \prod_{k=1}^{N} \phi_k(\omega) \tag{9}$$

where $\phi_k(\omega)$ is the ch. f. of q_k. From Weinstock [12, page 177], the ch. f. $\phi_k(\omega)$ is

$$\phi_k(\omega) = \left(1 - \frac{2i\omega}{d_k}\right)^{-1} \exp\left\{i\omega g_k^2 / \left(1 - \frac{2i\omega}{d_k}\right)\right\} \tag{10}$$

and, therefore,

$$\phi_S(\omega) = \prod_{k=1}^{N} \left(1 - \frac{2i\omega}{d_k}\right)^{-1} \exp\left\{i\omega g_k^2 / \left(1 - \frac{2i\omega}{d_k}\right)\right\}. \tag{11}$$

Inversion of $\phi_S(\omega)$ provides the probability density $f_S(s)$ of the random variable S. From this density we can determine the false-alarm and detection probabilities associated with a detection system which is based on the square-law integration of the outputs from a nonrecursive MTI. Inversion of (11) for the signal-present case (i.e., when g_k^2 is nonzero) has proven to be intractable. However, for the no-signal case ($g_k^2 = 0$), inversion can be accomplished as described in the next section.

BIAS LEVELS FOR SQUARE-LAW INTEGRATION

In this section we obtain an exact computational method for determining the bias levels (detection thresholds) to be used when a square-law integrator is applied to the output from a nonrecursive MTI.

When no signal is present at the MTI input, the means of X_k and Y_k (the real and imaginary parts of the MTI output) are zero. Thus, from (11), the ch. f. of S is

$$\phi_S(\omega) = \prod_{k=1}^{N} \left(1 - \frac{2i\omega}{d_k}\right)^{-1}. \tag{12}$$

When the eigenvalues $d_1, d_2, \ldots, d_N$ are all distinct (which is the case for the covariance matrices considered here), (12) can be inverted to give

$$f_S(s) = \frac{1}{2} \sum_{k=1}^{N} d_k P_k e^{-sd_k/2} \tag{13a}$$

where

$$P_k = \prod_{\substack{\ell=1 \\ \ell \neq k}}^{N} \left(1 - \frac{d_k}{d_\ell}\right)^{-1}. \tag{13b}$$

Therefore, the false-alarm probability PFA is given by

$$PFA = \sum_{k=1}^{N} P_k e^{-Td_k/2} \tag{14}$$

where T is the detection threshold. From (14) it follows that PFA is uniquely determined by the threshold T and the eigenvalues of A (which is the inverse of the covariance matrix R). However, R is the matrix

that is given (e.g., from equation (3)) and its inversion can be computationally difficult. Since the eigenvalues of A are reciprocals of the eigenvalues of R, it is not necessary to invert R. That is, it is only necessary to find the eigenvalues $\lambda_1, \lambda_2, \ldots, \lambda_N$ of R. (Note that $\lambda_k = d_k^{-1}$.) In terms of the eigenvalues of R, PFA becomes

$$PFA = \sum_{k=1}^{N} B_k e^{-T/2\lambda_k} \tag{15a}$$

where

$$B_k = \prod_{\substack{\ell=1 \\ \ell \neq k}}^{N} \left(1 - \frac{\lambda_\ell}{\lambda_k}\right)^{-1} . \tag{15b}$$

The computational method for obtaining the bias level $T_{N,PFA}$ is as follows: For each N, the eigenvalues $\lambda_1, \lambda_2, \ldots, \lambda_N$ are determined and the coefficients $B_1, B_2, \ldots, B_N$ are obtained from (15b). For each specified value of PFA, (15a) is solved for the bias level $T = T_{N,PFA}$ using Newton's method (or another numerical technique). The computations are illustrated in the next section where a particular example is discussed.

TWO-PULSE MTI FOLLOWED BY INCOHERENT INTEGRATION

For a two-pulse MTI (L = 2 in (3)) the covariance matrix R_N has the form

$$R_N = \begin{pmatrix} a & b & o & \cdots & o \\ b & a & b & o & \\ o & b & a & b & o \\ \vdots & o & \ddots & \ddots & \ddots \\ & & \ddots & \ddots & o \\ & & & \ddots & b \\ o & \cdots & o & b & a \end{pmatrix} \tag{16}$$

where $a = (W_1^2 + W_2^2)\,\sigma^2$ and $b = W_1 W_2 \sigma^2$. (The subscript N denotes the dimension of R and is also the number of MTI outputs incoherently integrated.) If binomial weights [13] are used (i.e., $W_1 = 1$, $W_2 = -1$), then $a = 2\sigma^2$ and $b = -\sigma^2$. In the following, a two-pulse MTI with binomial weights is assumed. Also, since the detection thresholds are normalized by the noise variance σ^2, no loss of generality occurs if we assume $\sigma^2 = 1$.

Bias levels

To obtain the eigenvalues of R_N, we compute the determinant of the matrix $R_N - \lambda I_N$ and find the roots of the polynomial equation

$$|R_N - \lambda I_N| = 0. \tag{17}$$

For the case being considered, the polynomials satisfy a recursive relation as a function of N. We make the change of variable $u = 2-\lambda$ in

(17) and denote by $D_N(u)$ the polynomial in u obtained from (17). The following recursive formula is easily verified:

$$
\begin{aligned}
&D_1(u) = u \\
&D_2(u) = u^2 - 1 \\
&\quad . \\
&\quad . \\
&\quad . \\
&D_N(u) = u\, D_{N-1}(u) - D_{N-2}(u) \\
&\qquad N = 3,4,\ldots
\end{aligned}
\tag{18}
$$

From (18) the derivative $D_N'(u)$ is also obtained recursively:

$$
\begin{aligned}
&D_1'(u) = 1 \\
&D_2'(u) = 2u \\
&\quad . \\
&\quad . \\
&\quad . \\
&D_N'(u) = u\, D_{N-1}'(u) - D_{N-2}'(u) + D_{N-1}(u) \\
&\qquad N = 3,4,\ldots
\end{aligned}
\tag{19}
$$

Using (18) and (19), Newton's method can be applied to compute the roots of (17).

Equations (18) and (19) were derived under the assumption that $a = 2$ and $b = -1$ in (16). However, it is easily shown that the solutions

of (17) in terms of the variable u defined above provide the most general solutions for any matrix of the form defined in (16). In (17), if we let $v = (a-\lambda)/|b|$, then the resulting polynomial in v is proportional to $D_N(v)$, where $D_N(\cdot)$ is defined in (18). Thus, the roots u_k, $k = 1,2, \ldots, N$, of (18) can be used to obtain the eigenvalues of any matrix R_N of the form (16) by defining $\lambda_k = a - |b|u_k$.

To illustrate the location of the eigenvalues of R_N, Figure 1 is a graph of $\lambda_1, \lambda_2, \ldots, \lambda_N$ as a function of N for N between 1 and 20. The continuous curves are obtained by connecting the m^{th} largest eigenvalue for each N. Because of symmetry about $\lambda = 2$, only the eigenvalues in the interval [2,4] are shown. (The eigenvalues for a particular value of N are found in Figure 1 at the intersection of the corresponding horizontal line with the continuous curves.)

Table 1 gives the bias levels required to obtain the indicated values of PFA for values of N between 2 and 39. Equations (18) and (19) were used to find the eigenvalues and (15) was used to determine T by the method described in the previous section.

Table 1 was computed for the case where a = 2 and b =-1 in (16). However, the results are more generally applicable. From the discussion above, the solutions of (18) can be used to determine the eigenvalues λ_k from $\lambda_k = a - |b|u_k$. If $a = 2|b|$, then $\lambda_k = |b|(2 - u_k)$ and the required threshold is $|b|T$, where T is the threshold given in Table 1. For example, if $\sigma^2 \neq 1$ (as was assumed previously) the required threshold is $T\sigma^2$, where σ^2 is the variance of the real and imaginary <u>inputs</u> to the MTI.

It should be noted that comparisons of the bias levels in Table 1 with Pachares' table [1] must take into account a difference in normalization

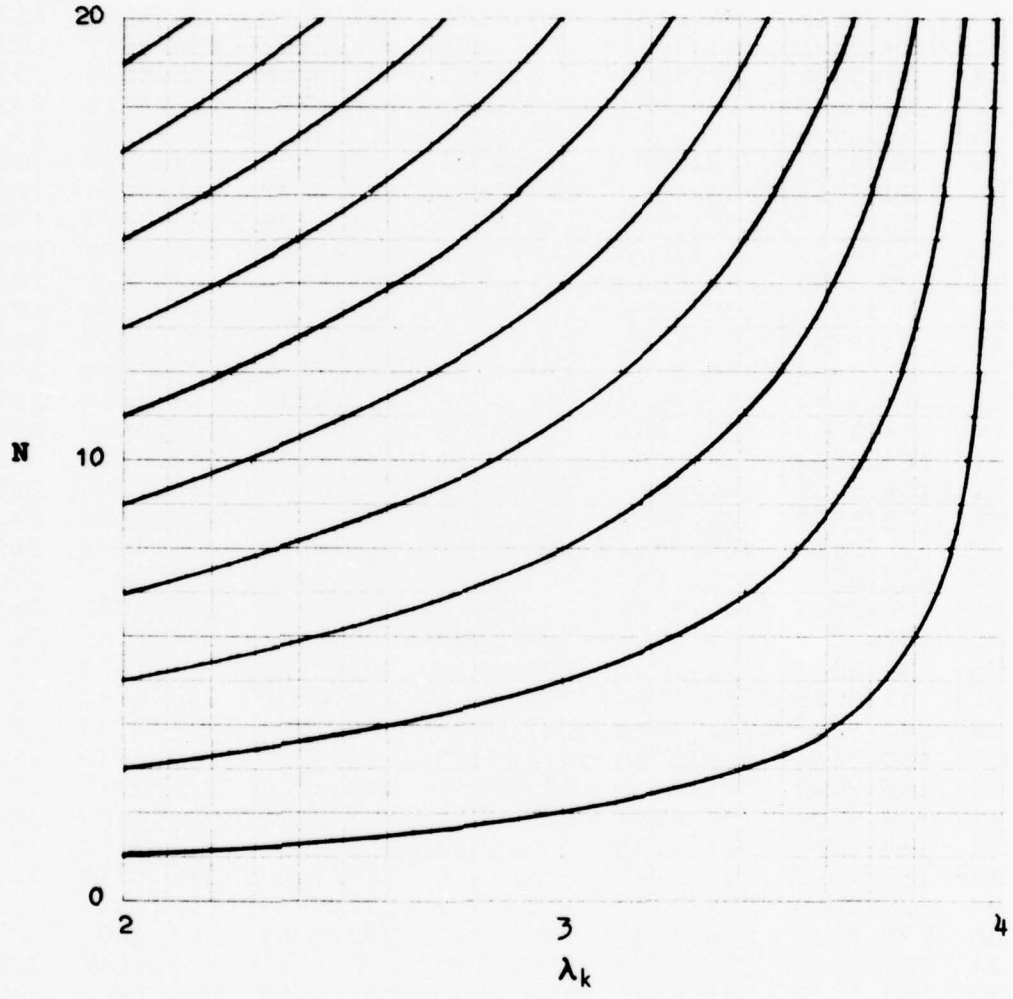

Figure 1. Location of the eigenvalues λ_k as a function of N.

N	$-\log_{10}$PFA 1	2	3	4	5	6
2	16.2394	30.0637	43.8793	57.6948	71.5103	85.3258
3	22.5577	38.6635	54.4551	70.1904	85.9148	101.6369
4	28.4521	46.2636	63.3186	80.1319	96.8537	113.5390
5	34.0875	53.3038	71.3648	88.9887	106.4079	123.7218
6	39.5437	59.9806	78.9033	97.2102	115.2028	133.0168
7	44.8678	66.3986	86.0883	104.9981	123.4918	141.7368
8	50.0896	72.6211	93.0118	112.4719	131.4218	150.0577
9	55.2293	78.6892	99.7301	119.7009	139.0738	158.0717
10	60.3013	84.6312	106.2821	126.7323	146.5028	165.8410
11	65.3162	90.4679	112.6956	133.5999	153.7474	173.4087
12	70.2822	96.1920	118.9632	140.2953	160.7979	180.7633
13	75.2057	101.8642	125.1612	146.9088	167.7576	188.0205
14	80.0919	107.4678	131.2694	153.4165	174.5986	195.1484
15	84.9448	113.0105	137.2983	159.8306	181.3347	202.1620
16	89.7680	118.5126	143.2727	166.1804	187.9989	209.0978
17	94.5644	123.9505	149.1648	172.4335	194.5545	215.9149
18	99.3363	129.3446	154.9998	178.6193	201.0347	222.6498
19	104.0860	134.6885	160.7703	184.7295	207.4302	229.2922
20	108.8152	140.0062	166.5055	190.7978	213.7786	235.8837
21	113.5255	145.2897	172.1961	196.8136	220.0682	242.4109
22	118.2183	150.5416	177.8454	202.7807	226.3031	248.8786
23	122.8948	155.7640	183.4564	208.7026	232.4873	255.2910
24	127.5562	160.9591	189.0316	214.5822	238.6241	261.6516
25	132.2034	166.1286	194.5734	220.4224	244.7165	267.9638
26	136.8373	171.2741	200.0837	226.2256	250.7673	274.2305
27	141.4586	176.3969	205.5646	231.9939	256.7788	280.4545
28	146.0681	181.4984	211.0176	237.7292	262.7534	286.6379
29	150.6665	186.5798	216.4443	243.4335	268.6930	292.7831
30	155.2543	191.6422	221.8461	249.1084	274.5995	298.8921
31	159.8320	196.6907	227.2291	254.7607	280.4805	304.9732
32	164.4002	201.7135	232.5798	260.3755	286.3194	311.0083
33	168.9593	206.7242	237.9140	265.9704	292.1358	317.0188
34	173.5098	211.7193	243.2279	271.5412	297.9251	322.9994
35	178.0520	216.6995	248.5222	277.0889	303.6882	328.9515
36	182.5862	221.6654	253.7978	282.6145	309.4265	334.8764
37	187.1129	226.6177	259.0556	288.1189	315.1409	340.7750
38	191.6324	231.5570	264.2963	293.6031	320.8324	346.6485
39	196.1449	236.4837	269.5205	299.0677	326.5019	352.4979

Table 1. Bias levels for square-law integration of N outputs from a binary-weighted, two-pulse nonrecursive MTI.

N	$-\log_{10}$PFA 7	8	9	10	11	12
2	99.1414	112.9569	126.7724	140.5879	154.4034	168.2189
3	117.3586	133.0801	148.8014	164.5227	180.2440	195.9652
4	130.2093	146.8733	163.5347	180.1950	196.8548	213.5144
5	140.9789	158.2045	175.4125	192.6106	209.8029	226.9920
6	150.7227	168.3606	185.9548	203.5204	221.0672	238.6014
7	159.8229	177.8028	195.7096	213.5649	231.3835	249.1755
8	168.4865	186.7724	204.9561	223.0651	241.1184	259.1296
9	176.8173	195.3849	213.8226	232.1629	250.4288	268.6371
10	184.8843	203.7164	222.3920	240.9486	259.4128	277.8040
11	192.7346	211.8180	230.7197	249.4816	268.1337	286.6982
12	200.3552	219.6747	238.7885	257.7427	276.5705	295.2966
13	207.8735	227.4256	246.7489	265.8937	284.8961	303.7831
14	215.2534	235.0303	254.5564	273.8856	293.0571	312.1002
15	222.5113	242.5062	262.2291	281.7376	301.0736	320.2684
16	229.6866	249.8958	269.8125	289.4980	308.9967	328.3418
17	236.7341	257.1496	277.2529	297.1086	316.7637	336.2535
18	243.6940	264.3109	284.5967	304.6191	324.4275	344.0591
19	250.5545	271.3669	291.8298	312.0140	331.9713	351.7407
20	257.3611	278.3665	299.0047	319.3492	339.4543	359.3606
21	264.0989	285.2936	306.1036	326.6057	346.8559	366.8970
22	270.7730	292.1534	313.1322	333.7890	354.1821	374.3557
23	277.3878	298.9505	320.0952	340.9042	361.4378	381.7420
24	283.9473	305.6891	326.9969	347.9557	368.6278	389.0607
25	290.4549	312.3729	333.8412	354.9475	375.7561	396.3159
26	296.9138	319.0051	340.6315	361.8832	382.8263	403.5113
27	303.3267	325.5887	347.3709	368.7659	389.8418	410.6504
28	309.6963	332.1264	354.0622	375.5985	396.8054	417.7361
29	316.0248	338.6207	360.7079	382.3837	403.7199	424.7712
30	322.3144	345.0737	367.3103	389.1238	410.5878	431.7582
31	328.5741	351.4951	373.8797	395.8297	417.4204	438.7090
32	334.7844	357.8640	380.3937	402.4776	424.1926	445.5973
33	340.9682	364.2049	386.8784	409.0951	430.9334	452.4534
34	347.1200	370.5118	393.3274	415.6753	437.6357	459.2697
35	353.2411	376.7862	399.7422	422.2199	444.3010	466.0478
36	359.3328	383.0294	406.1243	428.7303	450.9308	472.7893
37	365.3964	389.2427	412.4750	435.2080	457.5267	479.4957
38	371.4329	395.4273	418.7954	441.6541	464.0898	486.1684
39	377.4435	401.5843	425.0868	448.0699	470.6215	492.8086

Table 1. (Continued)

by a factor of two. That is, the variable considered by Pachares is one-half the sum of squares of input amplitudes (divided by the variance σ^2), while the variable considered here is not normalized by the factor one-half. (The change of variables used here to obtain (8) from (7) is $q_k = r_k^2$. The equivalent change of variables made by Pachares is $t = R_m^2/2\sigma^2$, using his notation.)

Figure 2 compares the thresholds required for a two-pulse MTI with those for no MTI. The curves for no MTI were obtained by doubling the values from Pachares' tables. It is interesting to note that for N larger than about 10 (and for the same PFA) the square root of the ratio of the two thresholds

$$\left(\frac{T_{NO\ MTI}}{T_{MTI}}\right)^{1/2}$$

is approximately 0.66, which is Ne/N as determined by Hall and Ward [3].

Characteristic function for the signal case

Suppose a signal of Doppler frequency f_d and amplitude G is present at the MTI input. Then, the real and imaginary parts of the outputs have mean values

$$\mu_k = -\left[2G \sin(\pi f_d/PRF)\right] \sin\left[2\pi f_d (k + \tfrac{1}{2})/PRF\right]$$

$$\gamma_k = \left[2G \sin(\pi f_d/PRF)\right] \cos\left[2\pi f_d (k + \tfrac{1}{2})/PRF\right] \qquad (20)$$

$$k = 1,2, \ldots, N$$

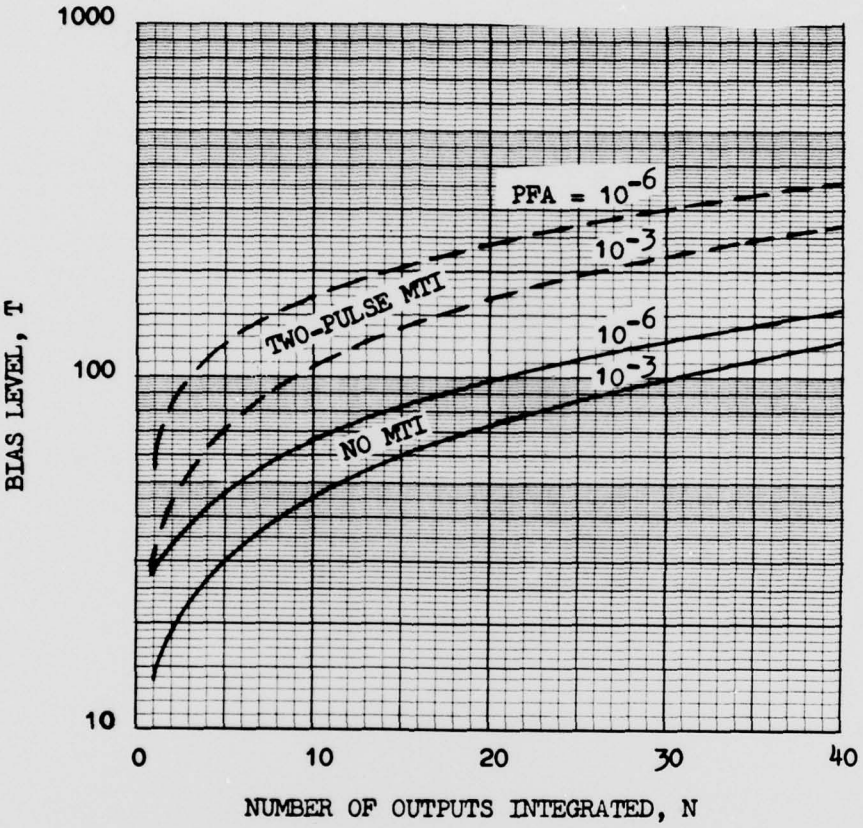

Figure 2. Comparison of the bias levels for a two-pulse MTI with those for no MTI.

To obtain the ch. f. $\phi_S(\omega)$ from (11), we must determine $g_k^2 \triangleq \alpha_k^2 + \beta_k^2$, where α_k and β_k are components of the vectors obtained from the transformations $\underline{\mu}' = T\underline{\alpha}'$ and $\underline{\gamma}' = T\underline{\beta}'$. It can be shown [11] that the matrix T has rows which are the unit-length eigenvectors $\underline{t}_k$ corresponding to the eigenvalues λ_k, $k = 1,2, \ldots, N$. Therefore, g_k^2 is given by

$$g_k^2 = (\underline{t}_k \underline{\mu}')^2 + (\underline{t}_k \underline{\gamma}')^2 \tag{21}$$

The eigenvectors $\underline{t}_k$ are obtained from the relationship

$$R_N \underline{t}_k' = \lambda_k \underline{t}_k' \tag{22}$$

and, for the covariance matrix R_N given by (16) (with $a = 2$ and $b = -1$), equation (22) leads to the relationship

$$t_{kj} = D_{j-1}(2 - \lambda_k)\, t_{k1} \tag{23a}$$

$$j = 2,3, \ldots, N$$

where

$$\underline{t}_k \triangleq (t_{k1}, t_{k2}, \ldots, t_{kN}) \tag{23b}$$

and $D_j(\cdot)$ is defined above in (17). In (23a), t_{k1} must be chosen such that $\underline{t}_k$ has unit length. Thus, we can define the eigenvector $\underline{t}_k$ from

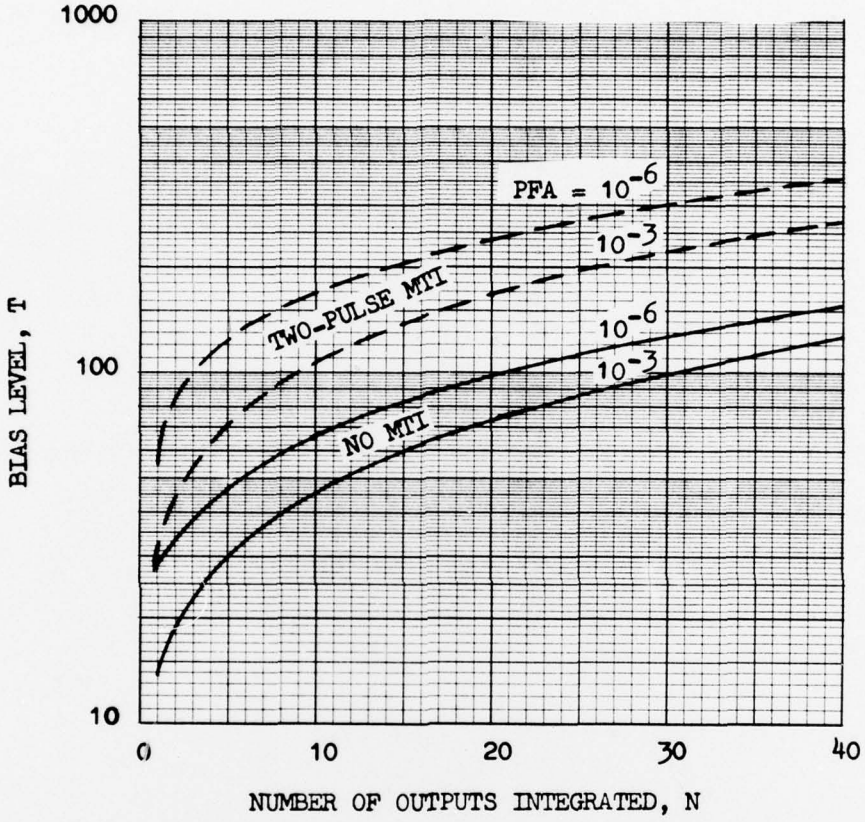

Figure 2. Comparison of the bias levels for a two-pulse MTI with those for no MTI.

To obtain the ch. f. $\phi_S(\omega)$ from (11), we must determine $g_k^2 \triangleq \alpha_k^2 + \beta_k^2$, where α_k and β_k are components of the vectors obtained from the transformations $\underline{\mu}' = T\underline{\alpha}'$ and $\underline{\gamma}' = T\underline{\beta}'$. It can be shown [11] that the matrix T has rows which are the unit-length eigenvectors $\underline{t}_k$ corresponding to the eigenvalues λ_k, $k = 1,2, \ldots, N$. Therefore, g_k^2 is given by

$$g_k^2 = (\underline{t}_k \underline{\mu}')^2 + (\underline{t}_k \underline{\gamma}')^2 \tag{21}$$

The eigenvectors $\underline{t}_k$ are obtained from the relationship

$$R_N \underline{t}_k' = \lambda_k \underline{t}_k' \tag{22}$$

and, for the covariance matrix R_N given by (16) (with $a = 2$ and $b = -1$), equation (22) leads to the relationship

$$t_{kj} = D_{j-1}(2 - \lambda_k)\, t_{k1} \tag{23a}$$

$$j = 2,3, \ldots, N$$

where

$$\underline{t}_k \triangleq (t_{k1}, t_{k2}, \ldots, t_{kN}) \tag{23b}$$

and $D_j(\cdot)$ is defined above in (17). In (23a), t_{k1} must be chosen such that $\underline{t}_k$ has unit length. Thus, we can define the eigenvector $\underline{t}_k$ from

$$t_{k1} = E_k^{-1}$$

$$t_{kj} = E_k^{-1} D_{j-1} (2 - \lambda_k) \qquad (24a)$$

$$j = 2,3, \ldots , N$$

where

$$E_k = \sqrt{1 + \sum_{\ell=1}^{N-1} D_\ell^2 (2 - \lambda_k)} \qquad (24b)$$

Now, rewriting (21), we have

$$g_k^2 = \alpha_k^2 + \beta_k^2 = \sum_{\ell=1}^{N} \sum_{m=1}^{N} (\mu_\ell \mu_m + \gamma_\ell \gamma_m) t_{k\ell} t_{km} \qquad (25a)$$

$$= 4G^2 \sin^2 (\pi f_d/PRF) \left(\sum_{\ell=1}^{N} t_{k\ell} \right)^2 \qquad (25b)$$

with (25b) obtained from (25a) using the relationship defined in (20). Equation (25b) can be further simplified. Note that

$$\sum_{\ell=1}^{N} t_{k\ell} = \underline{i}\, \underline{t}_k' \quad ,$$

where $\underline{i} \triangleq (1,1, \ldots , 1)$, and from (22):

$$\underline{i} R_N \underline{t}_k' = \lambda_k \underline{i}\, \underline{t}_k' = \lambda_k \sum_{\ell=1}^{N} t_{k\ell} \quad . \qquad (26)$$

But $\underline{i}\, R_N = (1,0, \ldots, 0,1)$, and (26) reduces to

$$\sum_{\ell=1}^{N} t_{k\ell} = (t_{k1} + t_{kN})/\lambda_k \tag{27}$$

Using (27), (25b), and (24) we have, finally,

$$g_k^2 = \frac{4G^2 \sin^2 (\pi f_d/PRF)}{\left[1 + \sum_{\ell=1}^{N-1} D_\ell^2 (2 - \lambda_k)\right]} \left(\frac{1 + D_{N-1} (2 - \lambda_k)}{\lambda_k}\right)^2 \tag{28}$$

APPLICATIONS TO OVERLAPPING DFT'S

The discussion above pertained to the square-law integration of the outputs from a nonrecursive MTI. We now consider briefly the application of the theory to square-law integration of coefficients of overlapping DFT's.

Signal detection is often accomplished by computing the discrete Fourier transform (DFT) of a sequence $G_0, G_1, \ldots, G_{M-1}$ of sensor outputs and comparing the magnitudes-squared of the DFT coefficients with a threshold. The length M of the DFT is determined by several factors, including the required signal resolution in the frequency domain [14].

To improve detection, it is sometimes necessary to perform incoherent integration of the DFT outputs. That is, a sequence of DFT's is computed and the magnitudes-squared of successive coefficients are

summed and compared with a threshold. The sequence of DFT's can be contiguous, as indicated in Figure 3a, or overlapping, as indicated in Figure 3b. When the DFT's are nonoverlapping, the quantities incoherently integrated are independent; however, when the DFT's are overlapping, the integration involves dependent (correlated) random variables. (Since we are dealing exclusively with Gaussian processes, correlation and dependence are used interchangeably.)

The correlation between coefficients of successive transforms depends both on the degree of overlap and on the "window-function" used in the DFT [14, page 56]. The q^{th} coefficient of the p^{th} DFT is defined as

$$F_{qp} = \sum_{k=0}^{M-1} W_k \, G_{k+p(M-r)} \, e^{-2\pi iqk/M} \qquad (29)$$

$$p = 0,1, \ldots ; \quad 0 \leq r \leq M - 1$$

where $\{W_k\}_{k=0}^{N-1}$ is the window function, and the parameter r defines the degree of overlap. (Note that r is defined differently here than by Harris [14, page 56].) Let the real and imaginary parts of F_{qp} be defined by

$$F_{qp} = X_{qp} + i \, Y_{qp} \qquad (30)$$

and assume that the inputs G_k, $k = 0,1, \ldots$, have real and imaginary parts that are IID Gaussian random variables with variance σ^2. Then, the covariance of X_{qp}, $X_{q,p+u}$ (and Y_{qp}, $Y_{q,p+u}$) is given by

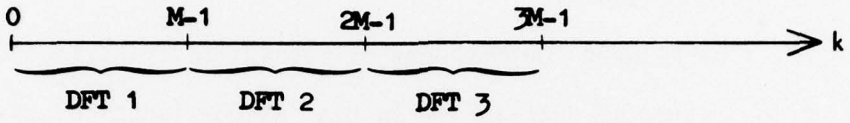

Figure 3a. Partitioning of input sequence for nonoverlapping DFT's.

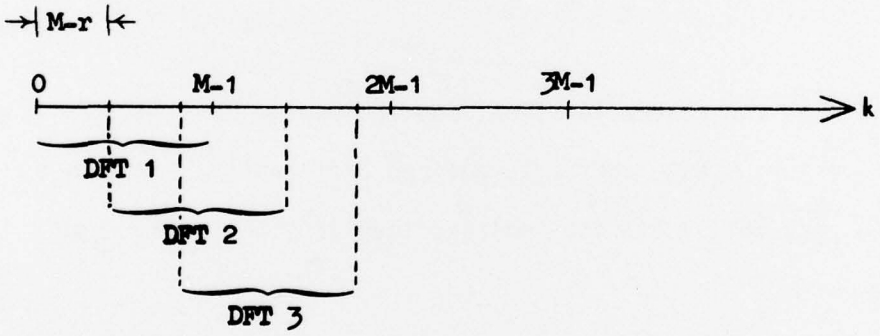

Figure 3b. Partitioning of input sequence for overlapping DFT's.

$$\phi_u = \sigma^2 \sum_{\ell=0}^{M-1+u(r-M)} W_\ell \, W_{\ell+u(M-r)} \;, \quad 0 \leq u \leq (M-1)/(M-r) \qquad (31)$$

$$= 0 \;, \text{ otherwise.}$$

(The index q has been suppressed in (31) since the covariance is independent of q.) Using (31), the covariance matrix of the real and imaginary parts of $F_{q0}, F_{q1}, \ldots, F_{q,N-1}$ can be determined and the previously derived theory can be applied to determine the bias levels to be used. If the presence of a signal is represented by having nonzero-mean inputs (such as defined by equation (20) in the previous section), the characteristic function for the signal-present case can also be derived.

If the signal to be detected is a narrowband Gaussian process, the presence of such a signal at the DFT input results in an increase in the variance of the real and imaginary parts of the DFT coefficient which corresponds to the center frequency of the input process.* Thus, for this coefficient the covariance when a signal is present is

$$\phi_{u,S} = \left(\frac{\sigma^2 + \sigma_S^2}{\sigma^2} \right) \phi_u, \qquad (32)$$

---

*Because of spectral leakage [14, page 52], the signal will increase the variance of all DFT coefficients. We assume that the bandwidth of the input process is narrow enough that only the DFT coefficient corresponding to the center frequency of the process will have a significant response.

where σ_S^2 is the variance of the signal component of the DFT input, and ϕ_u is the noise-only covariance given by (31). If the SNR ψ is defined such that $\psi = \sigma_S^2/\sigma^2$, the covariance $\phi_{u,S}$ is

$$\phi_{u,S} = (1+\psi)\ \phi_u \quad . \tag{33}$$

It follows that the probability of detection P_d can be computed from (15a) with T replaced by $T/(1+\psi)$.

As an example, for 50% overlap the covariance matrix has the form of (16) with $a = \phi_o$ and $b = \phi_1$, and recursive formulas similar to (18) and (19) can be derived. For a rectangular window (i.e., $W_k = 1$, $k = 0,1, \ldots, M-1$), $a = M\sigma^2$ and $b = \frac{M}{2}\sigma^2$. Thus, the thresholds tabulated in Table 1 are applicable if T is replaced by $MT\sigma^2/2$. This follows from the discussion of Table 1 above and the fact that $a = 2b$.

CONCLUSIONS AND DISCUSSION

The general theory has been given for obtaining the ch. f. of the sum of magnitudes squared of correlated circular-Gaussian random variables. This theory has been applied to the case of incoherent integration of the outputs from a nonrecursive MTI. In particular, the ch. f. has been determined explicitly for a two-pulse MTI, and the threshold levels which provide specified false-alarm probabilities have been determined and tabulated for several values of the number N of MTI outputs integrated.

The application of the theory to incoherent integration of the coefficients of overlapping DFT's has also been shown. It has been shown that

when the DFT's overlap by 50%, the tabulated thresholds for the two-pulse MTI can be used after appropriate scaling.

Detection probabilities have not been computed since inversion of the ch. f. for the signal-present case has, thus far, proven to be intractable. However, the technique of Helstrom [5] will be applied to estimate the detection probability and the results will be published later. These results will be compared with the estimates of Hall and Ward [3] and Trunk [2], and the degradation in performance due to noise correlation will be evaluated.

ACKNOWLEDGEMENTS

The authors acknowledge the support of Cliff Fowler and ORINCON Corporation in performing the computations described in this paper.

REFERENCES

1. Pachares, J., "A Table of Bias Levels Useful in Radar Detection Problems," IRE Trans. on Inf. Theory, Vol. IT-4, pp. 38-45, March 1958.

2. Trunk, G.V., "MTI Noise Integration Loss," IEEE Proceedings, Vol. 65, pp. 1620-1621, November 1977.

3. Hall, W.M., and H.R. Ward, "Signal-to-Noise Loss in Moving Target Indicator," IEEE Proceedings, Vol. 56, pp. 233-234, February 1968.

4. Kretschmer, F.F., Jr., "Correlation Effects of MTI Filters," IEEE Trans. on Aerospace and Electronic Systems, Vol. AES-13, pp. 321-322, May 1977.

5. Helstrom, C.W., "Approximate Evaluation of Detection Probabilities in Radar and Optical Communications," IEEE Trans. on Aerospace and Electronic Systems, Vol. AES-14, pp. 630-640, July 1978.

6. Helstrom, C.W., Statistical Theory of Signal Detection, 2nd ed., New York:Pergamon 1968.

7. Kac, M., and A.J.F. Siegert, "On the Theory of Noise in Radio Receivers with Square-Law Detectors," Journal of Applied Physics, Vol. 18, pp. 383-397, April 1947.

8. Emerson, R.C., "First Probability Densities for Receivers with Square Law Detectors," Journal of Applied Physics, Vol. 24, pp. 1168-1176, Sept. 1953.

9. Meyer, M.A., and D. Middleton, "On the Distributions of Signals and Noise After Rectification and Filtering," Journal of Applied Physics, Vol. 25, pp. 1037-1052, August 1954.

10. Kendall, M.G., and A. Stuart, The Advanced Theory of Statistics, Vol. 1, Hafner:New York, 1958.

11. Finkbeiner, D.T., II, Introduction to Matrices and Linear Transformations, Freeman:San Francisco, 1960.

12. Weinstock, W.W., "Probability Density and Distribution Functions," in Berkowitz, R.S., Modern Radar, Wiley:New York, 1965.

13. Nathanson, F.E., Radar Design Principles, McGraw-Hill:New York, 1969.

14. Harris, F.J., "On the Use of Windows for Harmonic Analysis with the Discrete Fourier Transform," IEEE Proceedings, Vol. 66, pp. 51-83, January 1978.